Journal of Power Sources 269 (2014) 747–754

Contents lists available at ScienceDirect

Journal of Power Sources

journal homepage: www.elsevier.com/locate/jpowsour

Lithium-active molybdenum trioxide coated $LiNi_{0.5}Co_{0.2}Mn_{0.3}O_2$ cathode material with enhanced electrochemical properties for lithium-ion batteries

Feng Wu [a, c], Jun Tian [a], Yuefeng Su [a, c, *], Yibiao Guan [b], Yi Jin [b], Zhao Wang [a], Tao He [a], Liying Bao [a, c], Shi Chen [a, c]

[a] School of Chemical Engineering and Environment, Beijing Institute of Technology, Beijing Key Laboratory of Environmental Science and Engineering, Beijing 100081, China
[b] China Electric Power Research Institute, Beijing 100192, China
[c] National Development Center of High Technology Green Materials, Beijing 100081, China

HIGHLIGHTS

- $LiNi_{0.5}Co_{0.2}Mn_{0.3}O_2$ were coated by MoO_3 via a wet coating process.
- Synthetic residue Li_2O/LiOH is eliminated by its reaction with MoO_3 to form Li_2MoO_4.
- Best improved electrochemical properties were obtained after 3 wt.% MoO_3 coating.

ARTICLE INFO

Article history:
Received 14 April 2014
Received in revised form
8 July 2014
Accepted 10 July 2014
Available online 18 July 2014

Keywords:
Lithium-ion batteries
Cathode material
Coating
Electrochemical properties

ABSTRACT

$LiNi_{0.5}Co_{0.2}Mn_{0.3}O_2$ cathode material was coated with MoO_3 via a wet coating process. X-ray diffraction patterns show that the coating surface is composed of MoO_3 and Li_2MoO_4. The 3 wt.% MoO_3 coated $LiNi_{0.5}Co_{0.2}Mn_{0.3}O_2$ cathode (Li_2MoO_4 is treated as equivalent mole of MoO_3) exhibits the best improved cycling performance. It performs a capacity retention of 90.9% after 100 cycles while that of the pristine material is only 82.8%. After being coated by 3 wt.% MoO_3, the rate performance is also greatly enhanced and the charge transfer resistance is greatly decreased. The improvement of electrochemical performance is related to the fact that the coating layer diminishes the side reactions between the cathode and the electrolyte.

1. Introduction

The growth of economy, population and fossil-energy consumption are impelling the interest of developing advanced power sources nowadays. High energy and high power density lithium-ion batteries are critically needed for applications in electric vehicles and renewable energy storage in smart grids [1–3]. Layered oxide $LiNi_xCo_yMn_zO_2$ are one of the commercialized cathode materials owing to its high discharge capacity and cycling performance. $LiNi_xCo_yMn_zO_2$, the redox couples of which are $Ni^{2+/3+}/Ni^{4+}$ and Co^{3+}/Co^{4+}, offers much higher discharge capacity compared with $LiCoO_2$. However, the relatively poor cycling performance at a high operating voltage (over 4.3 V) or high current density is one of its drawbacks. As an alternative, some efforts such as surface modification [4–8], ion doping [9–12] and fabrication of specific structures [13,14] have been demonstrated to be effective for enhancing its electrochemical performance.

Among the above mentioned approaches, surface modification by coating cathode materials with inert or active materials [15–18] has been extensively reported owing to its simplicity and effectivity. Many inorganic compounds have been reported to be coating layers to improve the electrochemical properties of $LiNi_xCo_yMn_zO_2$ as protective materials against corrosion from electrolyte. MoO_3 has relatively higher lithium-ion diffusivity than most metal oxides, metal phosphates and metal fluorides. It has been reported to be mixed with lithium-rich material to reduce its irreversible capacity loss during the first cycle by providing additional Li^+ insertion sites

* Corresponding author. School of Chemical Engineering and Environment, Beijing Institute of Technology, Beijing Key Laboratory of Environmental Science and Engineering, Beijing 100081, China. Tel.: +86 10 6891 8099; fax: +86 10 6891 8200.
E-mail address: suyuefeng@bit.edu.cn (Y. Su).

http://dx.doi.org/10.1016/j.jpowsour.2014.07.057
0378-7753/

or to be used as a lithium storage material [6,19,20]. In this work, $LiNi_{0.5}Co_{0.2}Mn_{0.3}O_2$ cathode material was coated with different amount of lithium-reactive MoO_3. Some amount of Li_2MoO_4 was found in the coating layer. The preparation, structure and electrochemical performance of the surface treated $LiNi_{0.5}Co_{0.2}Mn_{0.3}O_2$ was discussed compared with the pristine one.

2. Experimental section

2.1. Synthesis and characterization

$LiNi_{0.5}Co_{0.2}Mn_{0.3}O_2$ was prepared via a mixing "oxalate method". The aqueous solution with stoichiometric amount of nickel nitrate, cobalt nitrate and manganese nitrate was co-precipitated with ammonium oxalate aqueous solution by slowly pumping two solutions into a reaction tank, and the reaction solution was under vigorous stirring. During the precipitation, the pH value of the reaction solution was adjusted to 7.0 by adding ammonia. Precipitates were isolated by vacuum filtration and washed multiple times with distilled deionized water and then dried in the vacuum oven. The dried mixed oxalate precipitations were mixed with a required amount of $LiNO_3$ and then preliminarily fired at 500 °C for 6 h in air. Afterward, the precursors were pressed into pellets and calcined at 900 °C for 12 h. A wet coating process was used to prepare MoO_3-coated $LiNi_{0.5}Co_{0.2}Mn_{0.3}O_2$. A required amount of $(NH_4)_6Mo_7O_{24}\cdot 4H_2O$ were dissolved in deionized water accompanied by adding the as-prepared $LiNi_{0.5}Co_{0.2}Mn_{0.3}O_2$. The suspension was constantly stirred for 4 h with slow evaporation of water at 60 °C. Then the obtained product was calcined at 600 °C for 2 h. The 1 wt.%, 3 wt.% and 5 wt.% MoO_3 coated $LiNi_{0.5}Co_{0.2}Mn_{0.3}O_2$ were designed and labeled as MC1, MC2 and MC3, respectively.

The crystal structure of all the products was measured by X-ray powder diffraction (XRD, Rigaku UltimaIV-185) with Cu-Kα radiation at a scan rate of 4° 2θ/min. The morphology of the particles was performed by field emission scanning electron microscopy (FESEM, FEI QUANTA 250) and high-resolution transmission electron microscopy (TEM, FEI Tecnai G2 F20). And energy dispersive X-ray spectroscopy (EDX) was employed to analyze the surface composition and element distribution of cathode materials.

2.2. Electrochemical measurement

The working electrodes were prepared by a slurry coating procedure. The slurry consisted of 80 wt.% as-prepared material, 10 wt.% carbon conductive agent (carbon black) and 10 wt.% polyvinylidene fluoride (PVDF) in *N*-methyl pyrrolidone (NMP) solvent was coated onto aluminum foil. Then the coated aluminum foil was dried at 100 °C for 24 h and punched into discs of 15 mm in diameter. After that, the electrodes were assembled into CR2025 coin-type cells with Li electrodes and electrolyte (1 M $LiPF_6$ in EC:EMC:DMC = 1:1:1 in volume) in an Ar-filled glove box. The cells were cycled galvanostatically between 2.7 and 4.4 V (vs. Li/Li^+) at a desired current density at room temperature using CT2001A Land instrument. The cyclic voltammogram (CV) was operated between 2.5 and 4.5 V at a scan rate of 0.1 mV s^{-1}. The electrochemical impedance spectroscopy (EIS) measurements were conducted by a CHI660A impedance analyzer, using a frequency range of 100 kHz to 0.01 Hz.

3. Results and discussion

The XRD patterns of the pristine and MoO_3-coated $LiNi_{0.5}Co_{0.2}Mn_{0.3}O_2$ samples are exhibited in Fig. 1. All the patterns are well indexed with a layered hexagonal α-$NaFeO_2$ structure with space group $R\bar{3}m$ for the pristine sample $LiNi_{0.5}Co_{0.2}Mn_{0.3}O_2$. The clear splitting of (006)/(102) and (018)/(110) peaks demonstrates its high degree of crystallization [21]. For the MoO_3-coated samples, their main patterns are consistent with the pristine layered structure, but some minor peaks assigned to MoO_3 and Li_2MoO_4 emerged with the increase of the coating amount. These peaks can be clearly seen in the MC3 sample, but most of the peaks are so weak to be obviously seen in the XRD patterns of MC1 and MC2 samples due to the less content of Mo. Physical/chemical adsorption is ascribed to a small amount of synthetic residue Li_2O/LiOH on the surface, which causes a Li_2CO_3/LiOH layer after exposure to air and during cycling [22,23]. This layer is electrochemically inactive to lithium intercalation/de-intercalation, which is believed to be responsible for the capacity loss of the $LiNi_xCo_yMn_zO_2$ material. During the annealing process, the $(NH_4)_6Mo_7O_{24}$ was decomposed into MoO_3 that reacted with Li_2O/LiOH layer to form Li_2MoO_4. The consumption of Li_2O/LiOH could avoid the formation of Li_2CO_3/LiOH to prevent the moisture uptake. So minor amount of Li_2MoO_4 formed during the coating process could lead to a beneficial effect for the electrochemical performance of $LiNi_{0.5}Co_{0.2}Mn_{0.3}O_2$ to some extent.

The SEM images of the pristine and MoO_3-coated materials are shown in Fig. 2. It can be observed that all the samples display well-crystallized particles and have a similar morphology of ellipsoid-shaped grains in sub-micro size with a little agglomeration. The difference between the coated material and the pristine one can hardly be observed for that the coating layer is too thin.

The cycling performance and initial charge/discharge curves of all the samples at 0.2 C (1 C = 150 mAh g^{-1}) between 2.7 and 4.4 V at room temperature are present in Figs. 3 and 4, respectively. The relevant electrochemical data of them are shown in Table 1. The initial and 100th discharge capacities of the pristine $LiNi_{0.5}Co_{0.2}Mn_{0.3}O_2$ are 166.2 and 137.6 mAh g^{-1}, respectively, with a capacity retention of 82.8%. The pristine sample has an initial coulombic efficiency of 83.1%. For the MC1 sample, the cycling performance and initial charge/discharge performance are similar to that of the pristine one. However, when the coating amount of MoO_3 increases to 3 wt.% (MC2), although the initial discharge capacity (163.2 mAh g^{-1}) is lower than that of the pristine one, the discharge capacity after 100 cycles is greatly enhanced to 148.3 mAh g^{-1} (capacity retention 90.9%) and the initial coulombic efficiency (84.3%) is the highest among all the samples. The reason

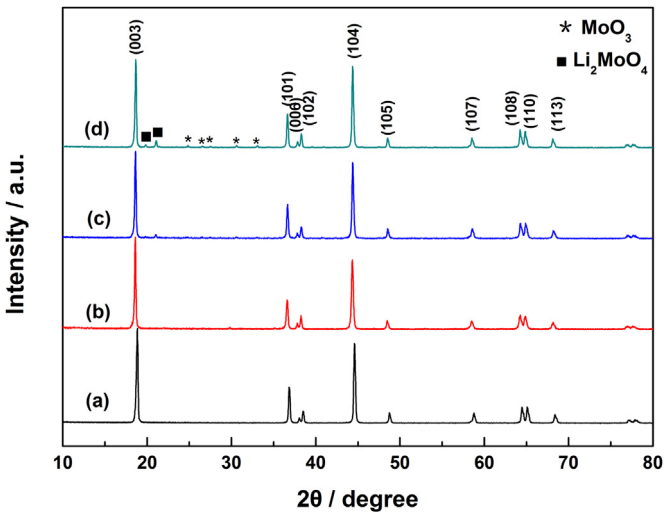

Fig. 1. XRD patterns of (a) the pristine $LiNi_{0.5}Co_{0.2}Mn_{0.3}O_2$ and MoO_3-coated samples: (b) MC1, (c) MC2, (d) MC3.

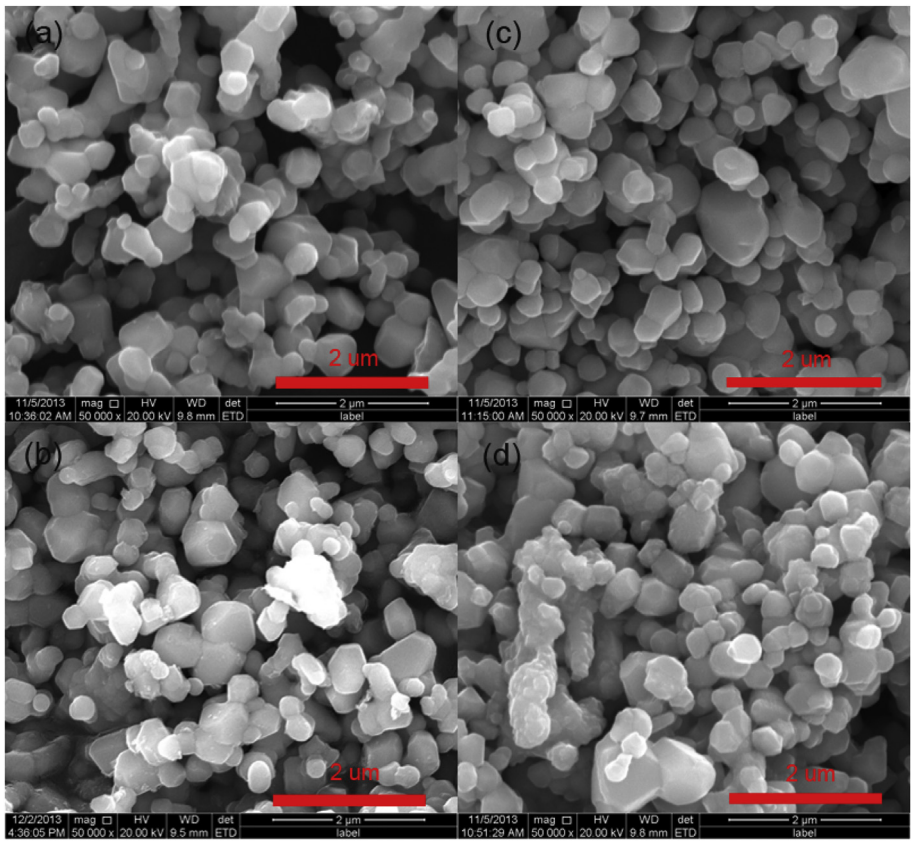

Fig. 2. SEM images of (a) the pristine and (b) MC1, (c) MC2, (d) MC3 powders.

may be that the MoO_3/Li_2MoO_4 layer avoids the formation of Li_2CO_3/LiOH layer as well as protects $LiNi_{0.5}Co_{0.2}Mn_{0.3}O_2$ from erosion by acid produced from electrolyte during cycling [24,25]. Conversely, as the coating concentration becomes higher, the presence of excess coating material between the particles could lower the particle-to-particle electronic conductivity [26]. Therefore, when the coating amount of MoO_3 increases to 5 wt.% (MC3), the initial coulombic efficiency and cycling performance are reduced to some extent compared with that of MC2.

The working voltages of $LiNi_xCo_yMn_zO_2$ material will decrease during cycling for the polarization caused by side reactions with the electrolytes [27,28]. Fig. 5 shows the charge and discharge voltage profiles of all the samples between 2.7 and 4.4 V at 0.2 C after 1st, 30th, 50th and 100th cycles, respectively. It is noted that the average working voltages of the MC2 sample decrease more slowly while cycling than that of the pristine $LiNi_{0.5}Co_{0.2}Mn_{0.3}O_2$. This result clearly indicates the 3 wt.% MoO_3/Li_2MoO_4 layer is very effective to block the side reactions with the electrolytes.

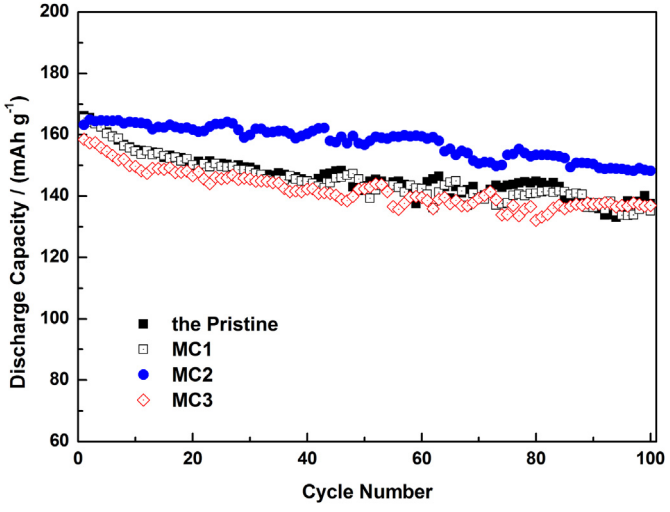

Fig. 3. Cycling performance of the pristine and MoO_3-coated $LiNi_{0.5}Co_{0.2}Mn_{0.3}O_2$ samples.

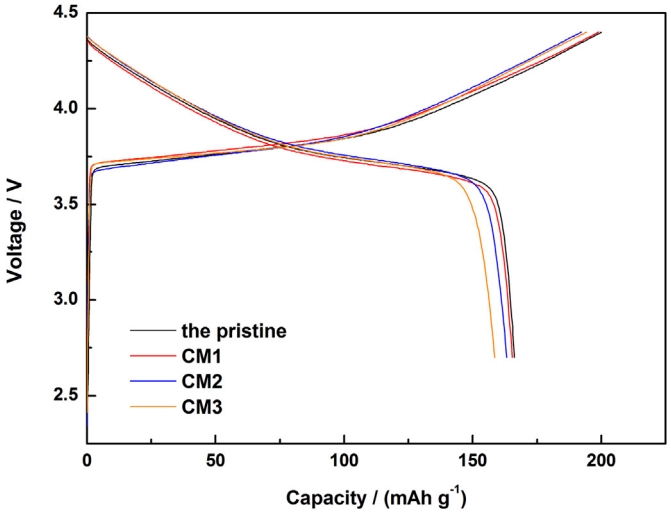

Fig. 4. The initial charge/discharge curves of (a) the pristine, (b) MC1, (c) MC2 and (d) MC3 samples.

Table 1
Electrochemical data of the pristine and MoO_3-coated $LiNi_{0.5}Co_{0.2}Mn_{0.3}O_2$ samples.

Sample	Initial charge capacity (mAh g^{-1})	Initial discharge capacity (mAh g^{-1})	Initial coulombic efficiency (%)	100th discharge capacity (mAh g^{-1})	Capacity retention after 100 cycles (%)
The pristine	200	166.2	83.1	137.6	82.8
CM1	199.0	165.3	83.1	135.2	81.8
CM2	192.3	163.2	84.9	148.3	90.9
CM3	194.3	158.5	81.5	136.9	86.3

Cyclic voltammograms of all the samples have been recorded at a sweep rate of 0.1 mV s^{-1} between 2.5 V and 4.5 V (Fig. 6) for the first three cycles to gather information about the individual redox process that occurs during the charge and discharge process. Only one anodic peak is found in the CV profiles of the pristine and MC2 samples, indicating Ni^{2+}/Ni^{4+} process is involved. In the previous research, only one anodic peak was observed upon the transition of Ni^{2+} to Ni^{4+} in the CV profiles [29,30]. This is because the Jahn–-Teller distortion of Ni^{3+} (d7) in NiO_6 octahedra leads to the direct oxidation of Ni^{2+} to Ni^{4+} [31].

For the pristine sample, the initial cathodic peak is centered at 4.056 V, corresponding to the delithiation of Li^+ from the lattice. The anodic peak is centered at 3.517 V, which corresponds to the intercalation of Li^+. The major cathodic and anodic peaks are assigned to the oxidation/reduction of Ni^{2+}/Ni^{4+} accompanied by the delithiation/lithiation process. The initial cathodic peak and anodic peak of the MC1 sample is 3.965 V and 3.596 V, respectively. Lower potential difference means that the polarization of MC1 sample is decreased compared with the pristine one. For the MC2 sample, the initial cathodic peak is centered at 3.864 V and the anodic peak is centered at 3.664 V. In the following scans, the major oxidation peak of the MC2 sample shifts to a lower voltage, and the CV peaks are steadier than that of the pristine. Obviously, the potential difference between the oxidation peak and the reduction peak of MC2 are much smaller than that of the pristine and MC1 samples, corresponding to lower interfacial polarization of cathodes. The MC3 sample has an initial cathodic peak of 3.850 V and an initial anodic peak of 3.670 V. The initial potential difference is a little smaller than that of the MC2 sample; however, the potential difference became larger in the following scans, and the stability of the peaks are weaker than the MC2 sample. All these results suggest that the reversibility of the 3 wt.% MoO_3-coated $LiNi_{0.5}Co_{0.2}Mn_{0.3}O_2$ cathode is better than the other samples. The coating layer protects the cathode material from erosion by acid produced from electrolyte during cycling. However, as the coating concentration becomes higher, the excess coating material between the particles could lower the particle-to-particle electronic conductivity. From the CV results, it is concluded MC2 sample has the lowest polarization for the reason that 3 wt.% is the proper coating amount. This can also be demonstrated in the EIS test.

Rate capability is one of the most significant electrochemical characteristics of the lithium rechargeable battery required for EVs and renewable energy storage application. Fig. 7a shows the rate discharging capacities of all the samples at the applied current densities. The simulation batteries based on the pristine and coated cathode materials are charged at 0.2 C and discharged at 0.2, 0.5, 1, 2, 5 C and finally 0.2 C, respectively, each for 5 cycles between 2.7 and 4.4 V. Although the pristine sample exhibits a considerable discharge capacity at 0.2 C, it presents serious capacity fading at high rates and maintains a capacity less than 90 mAh g^{-1} at 5 C. For the MoO_3-coated samples, their rate performance is improved on different levels, and all the coated samples possess higher capacities than the pristine one. The MC2 sample obtains the best capacity retention at high discharge rates among the MoO_3-coated materials. The representative discharging profiles of the pristine and MC2 samples at the same various C rates are illustrated in Fig. 7b. For the pristine sample, it yields initial discharge capacities of 167.3, 149.8, 134.9, 117.7, 84.2 mAh g^{-1} at 0.2, 0.5, 1, 2, 5 C, respectively. However, for the MC2 sample, the initial discharge capacities at 0.2, 0.5, 1, 2, 5 C are 162, 158, 150.4, 141.5, 124.4 mAh g^{-1}, respectively. Obviously, the rate capability of $LiNi_{0.5}Co_{0.2}Mn_{0.3}O_2$ are greatly enhanced with the appropriate MoO_3 coating amount of 3 wt.%.

The rate cycling performance of the pristine and the MC2 samples has been further determined by charging and discharging the electrodes at 1 C rate (as shown in Fig. 8a). The MC2 sample deliver an initial discharge capacity of 141.7 mAh g^{-1}, close to 141.7 mAh g^{-1} of the pristine one. However, the MC2 sample reveals a discharge capacity of 131.4 mAh g^{-1} with a capacity retention of 92.3% after 100 cycles, whereas the pristine one shows 118.1 mAh g^{-1} after 100 cycles. The discharging profiles (as shown in Fig. 8b) show that the discharge voltage platforms after different number of cycles are lower than that of the pristine one. These results suggest that the coating MoO_3/Li_2MoO_4 layer can protect the $LiNi_{0.5}Co_{0.2}Mn_{0.3}O_2$ particles from erosion by electrolyte even at high charge and discharge current density.

To determine the composition and distribution of chemical elements in all the samples, energy dispersive X-ray spectroscopy (EDS) has been carried out for each sample as presented in Fig. 9. Mapping of Mo has the same shape as the cathode material particle, indicating that there is a MoO_3/Li_2MoO_4 coating on the surface of the cathode material and the coating is uniform. This distribution,

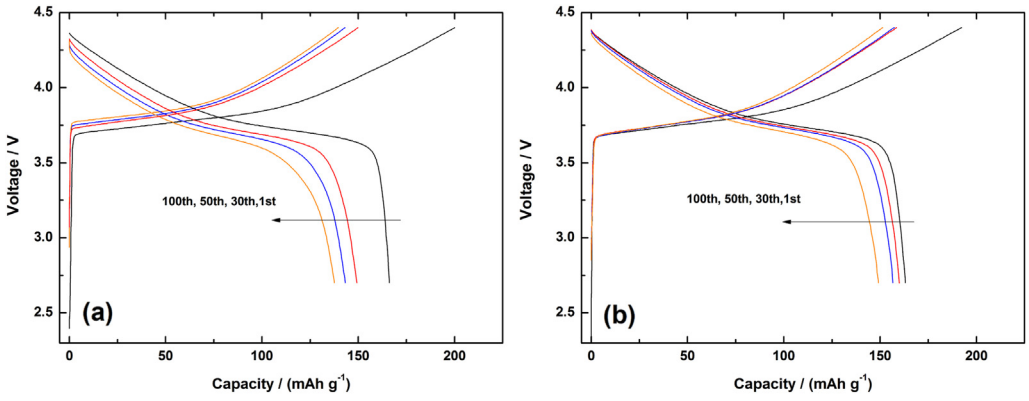

Fig. 5. Charge and discharge voltage profiles of (a) the pristine and (b) MC2 between 2.7 and 4.4 V after 1st, 30th, 50th and 100th cycles.

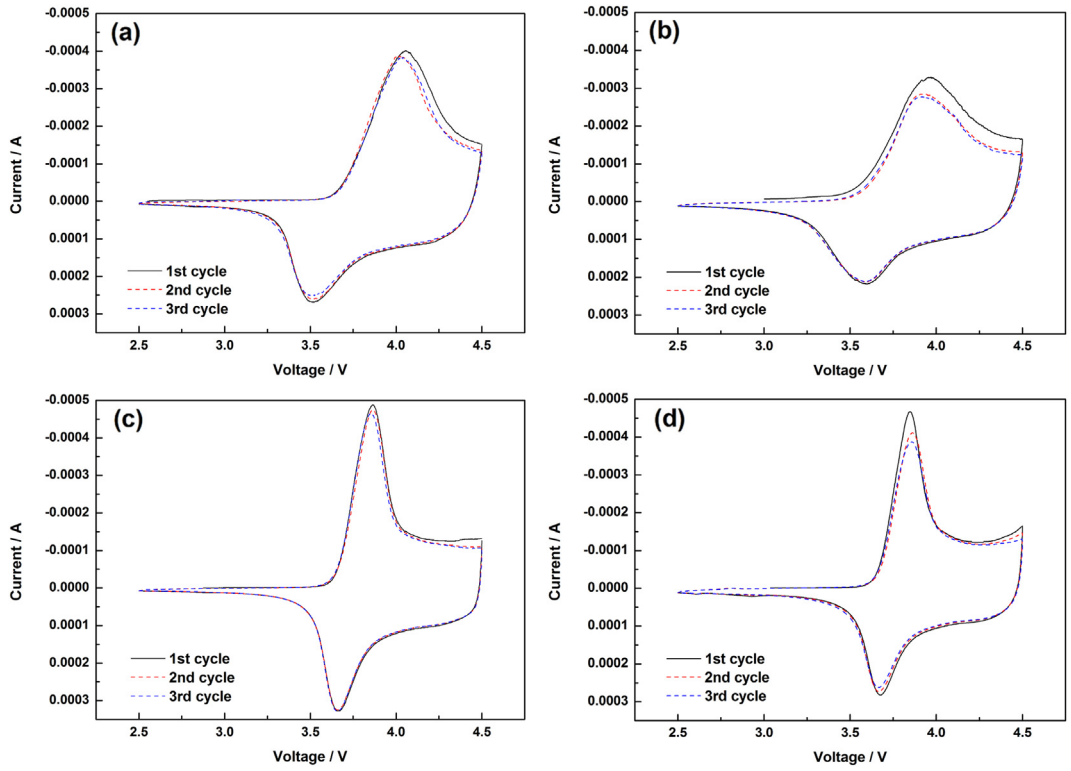

Fig. 6. Cyclic voltammograms of (a) the pristine (b) MC1, (c) MC2 and (d) MC3 samples.

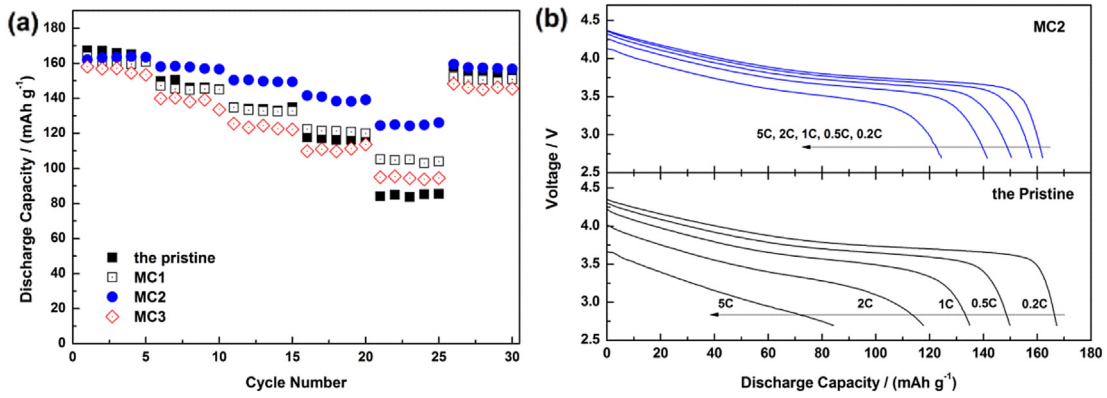

Fig. 7. The rate performance of all the samples: (a) discharge capacities under rates of 0.2 C, 0.5 C, 1 C, 2 C and 5 C in sequence for each 5 cycles and (b) discharging profiles for the pristine and CM2 samples at different rates.

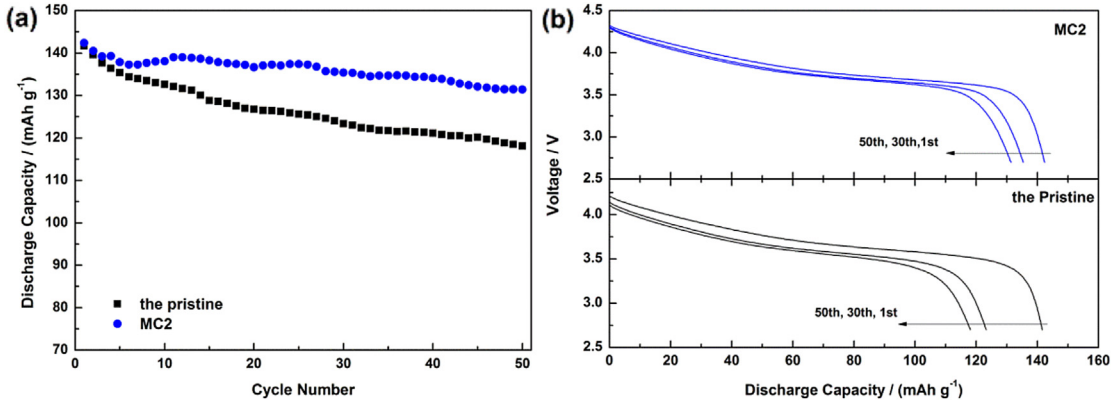

Fig. 8. (a) Cycling performance and (b) discharging profiles after 1st, 30th and 50th cycles at 1 C charge/discharge rate of the pristine and MC2 samples.

serving as a protection material would be favorable for improving rate and cycling performance of $LiNi_{0.5}Co_{0.2}Mn_{0.3}O_2$.

The TEM photographs of the pristine and MC2 particles are shown in Fig. 10. The particle fringe of the pristine material is smooth with nothing. Compared with the pristine one, the MoO_3/Li_2MoO_4 coating layer with a thickness of about 3–6 nm is clearly display as a fairly compact film on the surface of the $LiNi_{0.5}Co_{0.2}Mn_{0.3}O_2$ grains. From the above results, it can be concluded that the MoO_3/Li_2MoO_4 are only coated on the surface of $LiNi_{0.5}Co_{0.2}Mn_{0.3}O_2$ rather than entre the crystal structure.

To get insight into the origin of the improvement in electrochemical performance, electrochemical impedance spectra (EIS) of all the samples (as shown in Fig. 11) was measured after 1st, 30th, 50th and 100th cycles at 0.2 C rate. Each of the plots consist of a semicircle in the high-frequency region and a slope in the low-frequency region. Consequentially, the intercept of the semicircle at the highest frequency with the real axis (Z') refers to uncompensated ohmic resistance (R_s), the semicircle in the high-frequency region is related to the surface charge-transfer process (R_{ct}), and the slope in the low-frequency region corresponds to a Warburg diffusion process [32,33], the obtained EIS spectras are simulated using the equivalent circuit exhibited in Fig. 11e. The fitting results of R_s and R_{ct} for all the samples are shown in Table 2. It can be seen that all the samples show negligible ohmbic resistance of 2–9 Ω. The values of R_{ct} after the first cycle are close to each other. However, the MC2 sample has the lowest values of R_{ct} after 30th, 50th and 100th cycles. This suggests that the side reactions between cathode and electrolyte are greatly suppressed under the protection of the coating layer in the MC2 sample. Therefore, it can be concluded that the improvement of the electrochemical reaction activity contributes to the better cycling ability and rate capability of the 3 wt.% MO_3-coated material.

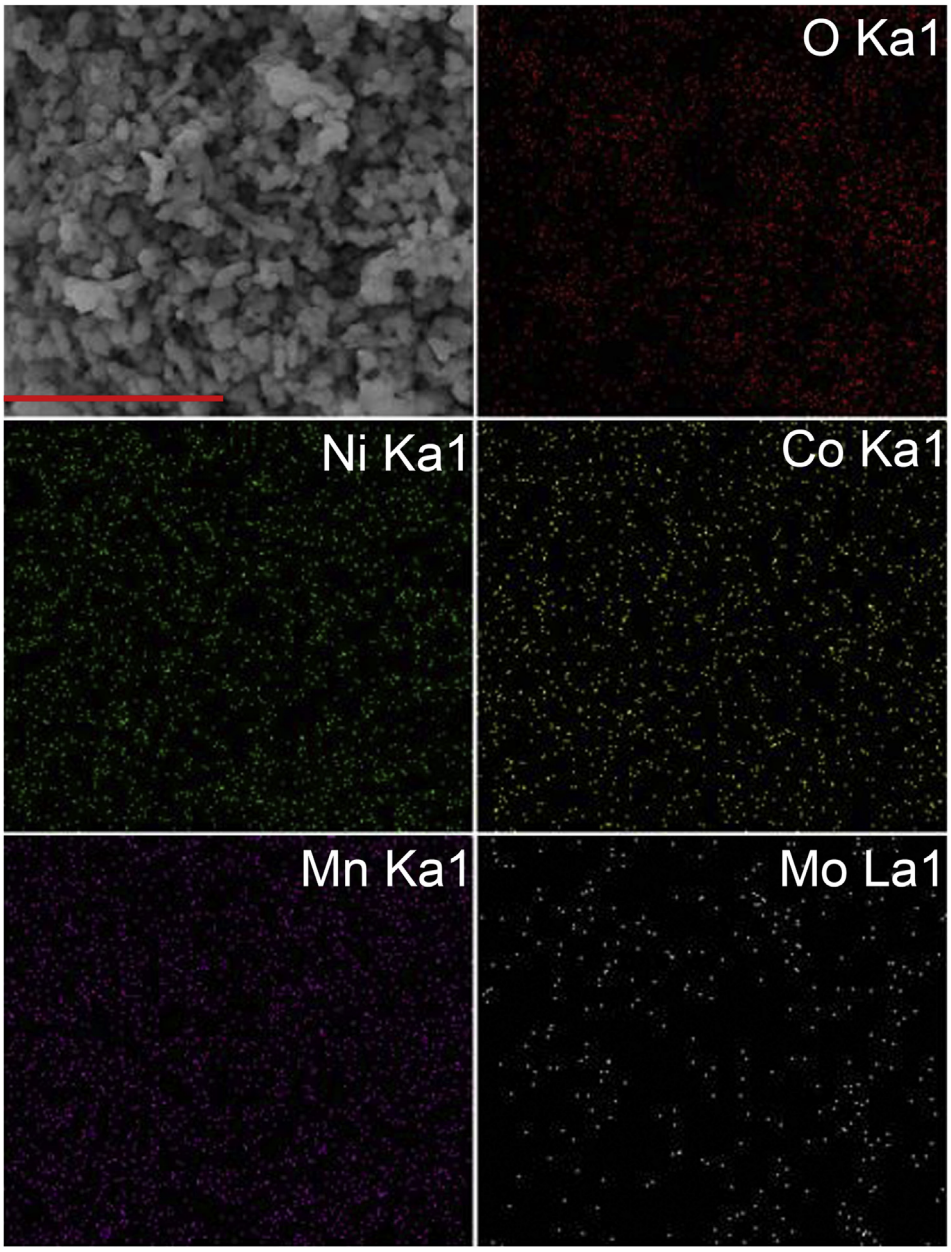

Fig. 9. EDS mapping of CM2 sample and the red bar corresponds to 7 μm. (For interpretation of the references to color in this figure legend, the reader is referred to the web version of this article.)

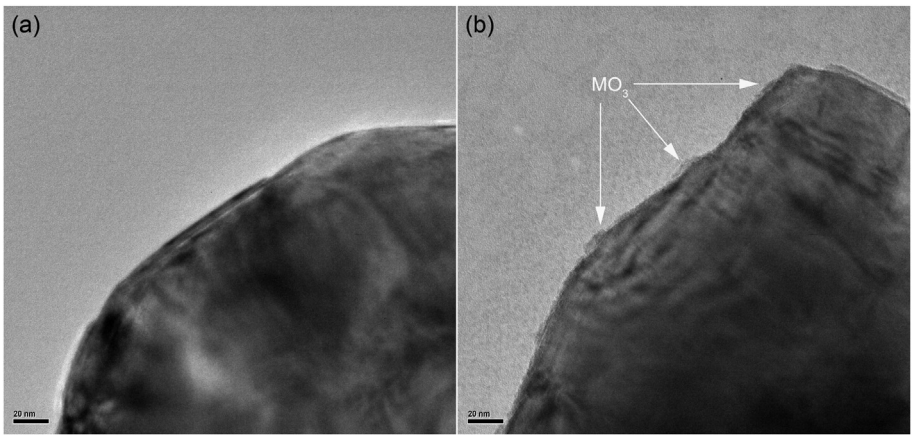

Fig. 10. TEM images of (a) the pristine and (b) the MC2 samples.

4. Conclusion

In our work, MoO_3-coated $LiNi_{0.5}Co_{0.2}Mn_{0.3}O_2$ was successfully prepared. The coating layer MoO_3/Li_2MoO_4 modifies the surface characteristics of electrode material and suppresses the side reactions between electrode and electrolyte. The 3 wt.% MoO_3-coated $LiNi_{0.5}Co_{0.2}Mn_{0.3}O_2$ exhibits enhanced cycling performance and rate capability compared to the pristine material. This

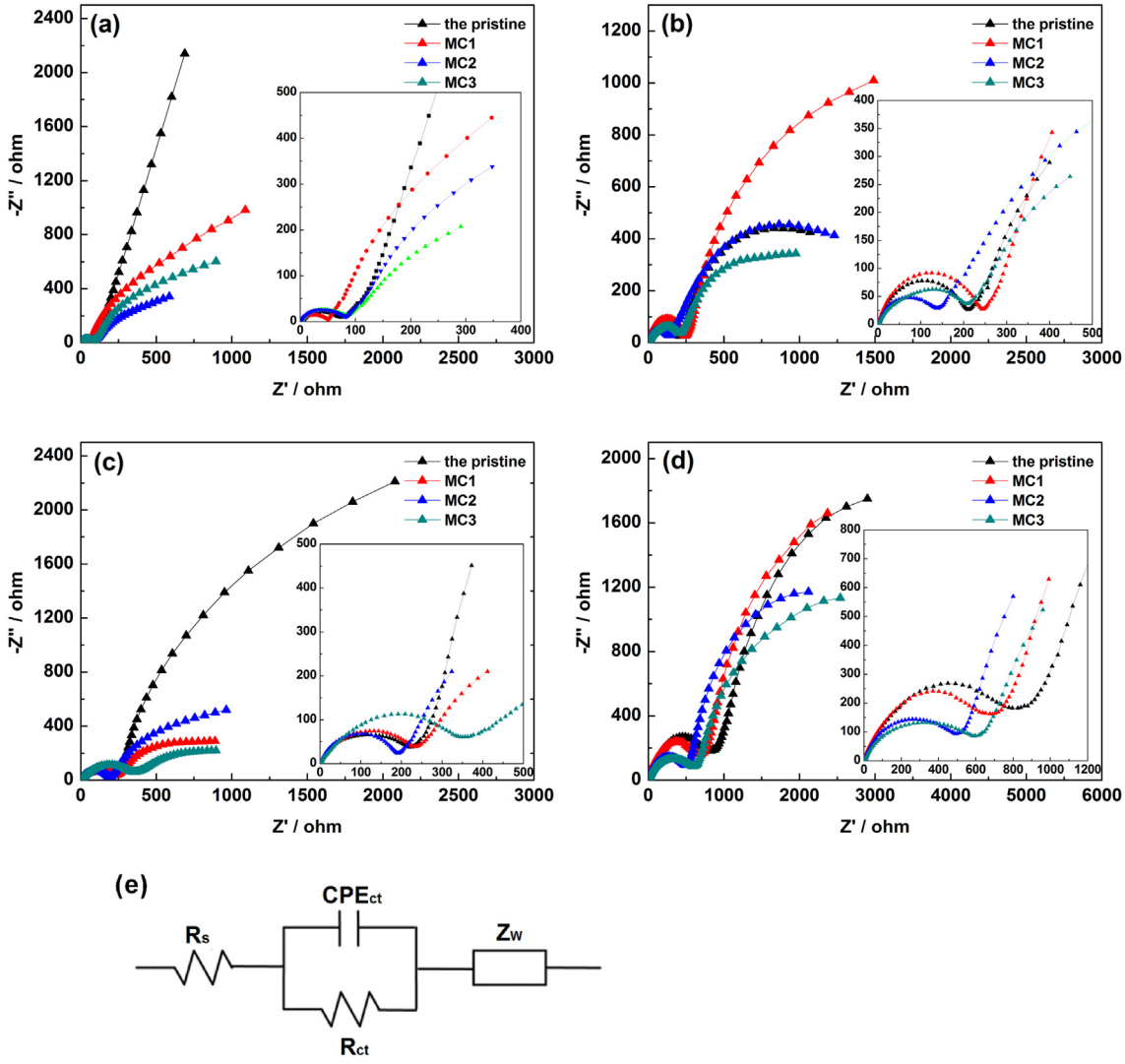

Fig. 11. Nyquist plots of all the samples after (a) 1st, (b) 30th, (c) 50th and (d) 100th cycle at equilibrium state and (e) the equivalent circuit model.

Table 2
Impedence data of the pristine and MoO_3-coated samples after different number of cycles at equilibrium state.

Cycle number	The pristine		MC1		MC2		MC3	
	R_s/ohm	R_{ct}/ohm	R_s/ohm	R_{ct}/ohm	R_s/ohm	R_{ct}/ohm	R_s/ohm	R_{ct}/ohm
1st	7.882	47.33	3.564	47.48	3.493	46.80	5.693	42.27
30th	2.529	164.1	4.602	141.6	3.539	100.0	2.170	174.6
50th	3.183	185.1	2.783	166.4	2.573	147.6	2.749	185.5
100th	4.033	511.8	3.307	419.7	7.099	314.3	8.515	377.2

enhancement is owing to the fact that the MoO_3/Li_2MoO_4 coating layer protects the material against erosion from electrolytes. In addition, the Li_2CO_3/LiOH layer which is detrimental to the electrochemical performance is also avoided to form due to the formation of Li_2MoO_4. Therefore, we conclude that an appropriate MoO_3/Li_2MoO_4 coating is an effective method to overcome the existing problems of layer $LiNi_xCo_yMn_zO_2$ cathode material for high power applications.

Acknowledgments

This work was supported by the National Basic Research Program of China (2009CB220100), the National Natural Science Foundation of China (51102018 and 21103011), Program for New Century Excellent Talents in University (NCET-13-0044), the BIT Scientific and Technological Innovation Project (2013CX01003) and Technology Project of State Grid Corporation (DG71-13-033).

References

[1] M. Armand, J.M. Tarascon, Nature 451 (2008) 652–657.
[2] B. Dunn, H. Kamath, J.-M. Tarascon, Science 334 (2011) 928–935.
[3] L. Su, Y. Jing, Z. Zhou, Nanoscale 3 (2011) 3967–3983.
[4] S.J. Shi, J.P. Tu, Y.Y. Tang, Y.Q. Zhang, X.Y. Liu, X.L. Wang, C.D. Gu, J. Power Sources 225 (2013) 338–346.
[5] X.H. Xiong, Z.X. Wang, X. Yin, H.J. Guo, X.H. Li, Mater. Lett. 110 (2013) 4–9.
[6] F. Wu, Z. Wang, Y.F. Su, N. Yan, L.Y. Bao, S. Chen, J. Power Sources 247 (2014) 20–25.
[7] B. Huang, X.H. Li, Z.X. Wang, H.J. Guo, Z.J. He, R.H. Wang, J.X. Wang, X.H. Xiong, Mater. Lett. 115 (2014) 49–52.
[8] Y.L. Yao, H.C. Liu, G.C. Li, H.R. Peng, K.Z. Chen, Electrochim. Acta 113 (2013) 340–345.
[9] C.X. Gong, W.X. Lv, L.M. Qu, O.E. Bankole, G.H. Li, R. Zhang, M. Hu, L.X. Lei, J. Power Sources 247 (2014) 151–155.
[10] H. Konishi, M. Yoshikawa, T. Hirano, J. Power Sources 244 (2013) 23–28.
[11] S.X. Liu, H.L. Zhang, Rare Metal. Mat. Eng. 42 (2013) 296–300.
[12] N. Li, R. An, Y. Su, F. Wu, L. Bao, L. Chen, Y. Zheng, H. Shou, S. Chen, J. Mater. Chem. A 1 (2013) 9760–9767.
[13] Y. Cho, P. Oh, J. Cho, Nano Lett. 13 (2013) 1145–1152.
[14] Y.K. Sun, Z. Chen, H.J. Noh, D.J. Lee, H.G. Jung, Y. Ren, S. Wang, C.S. Yoon, S.T. Myung, K. Amine, Nat. Mater. 11 (2012) 942–947.
[15] X.F. Li, J. Liu, X.B. Meng, Y.J. Tang, M.N. Banis, J.L. Yang, Y.H. Hu, R.Y. Li, M. Cai, X.L. Sun, J. Power Sources 247 (2014) 57–69.
[16] J. Lu, Q. Peng, W. Wang, C. Nan, L. Li, Y. Li, J. Am. Chem. Soc. 135 (2013) 1649–1652.
[17] G.R. Li, X. Feng, Y. Ding, S.H. Ye, X.P. Gao, Electrochim. Acta 78 (2012) 308–315.
[18] T. Liu, S.-X. Zhao, K. Wang, C.-W. Nan, Electrochim. Acta 85 (2012) 605–611.
[19] J.F. Ni, G.B. Wang, J. Yang, D.L. Gao, J.T. Chen, L.J. Gao, Y. Li, J. Power Sources 247 (2014) 90–94.
[20] M. Kovendhan, D.P. Joseph, P. Manimuthu, S. Sambasivam, S.N. Karthick, K. Vijayarangamuthu, A. Sendilkumar, K. Asokan, H.J. Kim, B.C. Choi, C. Venkateswaran, R. Mohan, Appl. Surf. Sci. 284 (2013) 624–633.
[21] D.-C. Li, T. Muta, L.-Q. Zhang, M. Yoshio, H. Noguchi, J. Power Sources 132 (2004) 150–155.
[22] J. Kim, Y.S. Hong, K.S. Ryu, M.G. Kim, J. Cho, Electrochem. Solid-State Lett. 9 (2006) A19–A23.
[23] H.S. Liu, Y. Yang, J.J. Zhang, J. Power Sources 162 (2006) 644–650.
[24] Z. Chen, Y. Qin, K. Armine, Y.K. Sun, J. Mater. Chem. 20 (2010) 7606–7612.
[25] S.-T. Myung, K. Armine, Y.-K. Sun, J. Mater. Chem. 20 (2010) 7074–7095.
[26] G.T.K. Fey, C.Z. Lu, T.P. Kumar, Y.C. Chang, Surf. Coat. Technol. 199 (2005) 22–31.
[27] R. Jorn, R. Kumar, D.P. Abraham, G.A. Voth, J. Phys. Chem. C 117 (2013) 3747–3761.
[28] N.S. Norberg, S.F. Lux, R. Kostecki, Electrochem. Commun. 34 (2013) 29–32.
[29] J. Choi, A. Manthiram, Electrochem. Solid-State Lett. 8 (2005) C102–C105.
[30] S.H. Park, C.S. Yoon, S.G. Kang, H.S. Kim, S.I. Moon, Y.K. Sun, Electrochim. Acta 49 (2004) 557–563.
[31] J. Ni, H. Zhou, J. Chen, X. Zhang, Electrochim. Acta 53 (2008) 3075–3083.
[32] J. Liu, A. Manthiram, J. Mater. Chem. 20 (2010) 3961–3967.
[33] P. Li, H. Liu, B. Lu, Y. Wei, J. Phys. Chem. C 114 (2010) 21132–21137.